Mechanisms of ginsenoside Rg1 in preventing ETEC-induced diarrhea: Maintaining ileal integrity and eliminating inflammation

Jian Kang
South China Agricultural University https://orcid.org/0000-0002-6447-223X
Qin Ai
Wen's Foodstuffs Group Cp., Ltd
Yanhong Zhou
South China Agricultural University
Chunyang Zhu
South China Agricultural University
Binghu Fang (fangbh@scau.edu.cn)
South China Agricultural University https://orcid.org/0000-0003-4858-9304

Research

Keywords: Ginsenoside, Rg1, ETEC, Mice, Diarrhea, Inflammation, Proteomics

Posted Date: November 19th, 2020

DOI: https://doi.org/10.21203/rs.3.rs-111025/v1

Abstract

Background: Enterotoxigenic *Escherichia coli* (ETEC) can cause severe watery diarrhea and rapid dehydration or death of newborn animals, resulting in significant economic losses of animal farms around the world. The endotoxin produced by ETEC usually causes inflammation and damage to the integrity of the intestinal mucosa, which leads to the destruction of intestinal homeostasis. To date, ETEC infections have been treated widely using drugs and antibiotics. Unfortunately, after high-dose or long-term antibiotic treatment, ETEC might develop drug or antibiotic resistance, and the animal products might also contain their residues. Therefore, the development of antibiotic substitutes has been explored widely by scholars. The main phytocomponent of Ginseng is ginsenoside Rg1 (GRg1), which has shown anti-inflammatory properties in animal models and cell lines.

Methods: Mice were infected with ETEC after 14 days of treatment with different doses of GRg1, and the diarrhea index, ileal pathological changes, and inflammatory factors in plasma were compared. Changes to the proteins in the ileum were assessed using proteomics.

Results: ETEC challenge not only increased the serum content of inflammatory cytokines, such as interleukin (IL) 1β, IL6, and tumor necrosis factor alpha (TNFα), ($P < 0.05$), but also induced pathological changes in the ileum such as reduction of villus height, crypt depth ($P < 0.05$), and inflammatory cell infiltration. However, different doses of GRg1 treatment significantly reversed the above changes, with no significant dose dependence ($P > 0.05$). Proteomic analysis identified 55 differentially abundant proteins in the ileum of ETEC-infected mice treated with and without GRg1. Bioinformatic analysis indicated that these proteins were involved in 15 signaling pathways, particularly, the complement and coagulation cascade pathway and the platelet activation pathway. Western blotting identified that the key proteins complement C3, fibrinogen (Fg)A, FgB and FgG in these signaling pathways were significantly downregulated by GRg1 ($P < 0.05$), which was consistent with the proteomic analysis.

Conclusion: GRg1 alleviates ETEC diarrhea in mice by eliminating the infection-related inflammatory reaction and maintaining the integrity of intestinal mucosa.

1. Background

Enterotoxigenic Escherichia coli (ETEC) infection of animals results in severe diarrhea and rapid dehydration. ETEC infects mammals such as humans, mice, and pigs [1, 2]. ETEC adhere to the microvilli of the small intestine, resulting in lesions, and secrete enterotoxins that act locally on enterocytes. These enterotoxins cause inflammation of the intestinal mucosa, destroy the integrity of tight junctions, and induce apoptosis of epithelial cells [3], subsequently leading to intestinal homeostasis disruption and intestinal barrier function damage. To date ETEC infections have been treated widely using drugs and antibiotics. Unfortunately, after high-dose or long-term treatment, ETEC might develop drug or antibiotic resistance, and the animal products might also contain their residues. For example, to treat gram-negative bacterial infections, tetracyclines (Doxycycline), aminoglycosides (gentamicin, streptomycin), and

polypeptides (colistin) are prescribed frequently [4–7]. Unfortunately, these drugs are associated with adverse drug reactions (ADRs), including hypopsia, nausea, diarrhea and allergy [4–7]. Therefore, scholars are actively seeking alternative treatments for ETEC.

Ginseng is widely used in traditional Chinese medicine because of its anti-oxidant, anti-aging, and anti-inflammatory effects [10, 11]. Ginseng contains a variety of active ingredients, including ginsenosides, fatty acids, polysaccharides, and mineral oils [12], the pharmacological effects of which are mainly attributed to ginsenosides [13]. To date, more than 30 ginsenosides have been identified [13], such as RE, Rd, Rb1/2, Rg3, and Rh2/3 [15]. Among them, ginsenoside Rg1 (GRg1) is the most active and abundant steroidal saponin, with a similar structure to other steroidal hormones [16]. GRg1 has many pharmacological effects, such as anti-infertility, antitumor, antimicrobial, immunomodulatory, antiproliferative, and antioxidant [17, 18]. In addition, recent studies have pointed out that GRg1, as an effective antioxidant stress substance, can reduce oxidative damage to the liver [19–21]. More importantly, in animal models and cell lines, GRg1 showed strong anti-inflammatory effects [22–24].

Thus, the present study aimed to investigate the effects of GRg1 on plasma inflammatory factors, ileum morphology, and ileum protein levels, in mice with ETEC diarrhea, and to evaluate its therapeutic effect and mechanism on ETEC diarrhea mice.

2. Methods

2.1 Materials

High performance liquid chromatography (HPLC) grade GRg1 (22427-39-0, was obtained from Shanghai Macklin Biochemical Co., Ltd (Shanghai, China). The ETEC strain was purchased from the China Center of Industrial Culture Collection (CICC 10413). Mouse β-actin antibodies (catalog number D191047) were obtained from Sangon Biotech Co., Ltd. (Shanghai, China). Rabbit antibodies recognizing fibrinogen (Fg)A (catalog number 20645-1-AP), FgB (catalog number 16747-1-AP), FgG (catalog number 15841-1-AP), and complement C3 (catalog number 21337-1-AP) were obtained from Proteintech Group, Inc. (Wuhan, China). Enzyme-linked immunosorbent assay (ELISA) kits for tumor necrosis factor alpha (TNFα) (catalog number ml002859), interleukin (IL)6 (catalog number ml002293) and IL1β (catalog number ml063132) were obtained from Shanghai MLBIO Biotechnology Co. Ltd. (Shanghai, China).

2.2 Animal study

Specific pathogen-free (SPF) 20-day-old KM mice were kept in single cages under a 12 h light/dark cycle, with constant temperature (20–25 °C) and humidity (40–70%), with *ad libitum* access to food and water for 7 days. No feeding and drinking were allowed 12 hours before the experiment. The Animal Protection and Use Committee of South China Agricultural University approved all the animal experiments. The study was performed following the “Guidelines for the Care and Use of Laboratory Animals” from the National Institutes of Health (NIH, Bethesda, MD, USA).

Sixty healthy mice were divided randomly into five groups of 12 mice each (n = 12). Mice were treated with GRg1 at 50 mg/kg (LD group), 100 mg/kg (MD group), and 150 mg/kg (HD group) for 14 days

(orally). After 14 days of continuous treatment, the ETEC infection (Model) group and three GRg1 treatment groups were injected intraperitoneally with 0.2 mL ETEC bacterial solution at 3×10^7 colony forming units (CFU)/mL, and the Normal (control) group was injected intraperitoneally with the same volume of normal saline. After inoculation of ETEC, mice were fed in single cages. Filter paper was laid at the bottom of each cage and the health status of the mice in each group was observed. All filter papers were replaced when the mice had diarrhea symptoms (such as loose stools, signs of depression, piling up, closing eyes, or drooping head). Thereafter, to avoid contamination of feces by urine, the filter paper was changed every time the mice urinated or defecated, and the grade of loose stool was recorded for 6 hours. We defined the diarrhea index = the sum of the loose stools grades per mouse/total number of defecations per mouse, and regarded it as the standard for judging the degree of diarrhea in mice. The loose stools grade represented the degree of defecation of each animal, and was graded according to the diameter of the stain area formed by the loose feces polluting the filter paper, as shown in Table 1.

After 6 hours of recording, plasma samples were collected for ELISA detection. After euthanasia, the duodenum of mice was excised. Part of the duodenum was subjected to hematoxylin and eosin (H & E) staining. The other part was stored in a freezer at −80 °C.

Table 1
Criteria for judging the loose stool grade

Diameter of the stain area (cm)	Loose stool grade
Diameter ≤ 1	1
1 Diameter ≤ 2	2
2 Diameter ≤ 3	3
Diameter 3	4

2.3 Histopathological analysis

The ileum samples on slides were fixed in formalin and then rinsed with water to remove the excess fixative. A graded series of ethyl alcohol was used to dehydrate the samples, which were cleared using xylene, and then paraffin wax-embedded. The samples were stained with H & E for 12 h at room temperature. Finally, the stained tissue on the slides were examined under a light microscope (BX43; Olympus Co., Tokyo, Japan) at 200 × magnification and photographed using the attached digital camera. The images were examined by an expert pathologist to determine any morphological changes to the ileum [25]. The villi height and crypt depth were measured by Image-Pro Plus 6.0.

2.4 Sample preparation for proteomic analysis

The frozen samples were treated with liquid nitrogen and homogenized in a cryogenic mill. Subsequently, 600 μL of phenol extraction solution and a final concentration 1 mM of phenylmethylsulfonyl fluoride (PMSF) were added. The mixture was sonicated on ice, added with an equal volume of phenol-Tris-HCl (pH 7.8) saturated solution, and then centrifuged at 7000 × *g* for 10 min at 4 °C to collect the supernatant, which was added with five volumes of pre-cooled ammonium acetate in methanol (0.1 M), and stored

overnight at −20 °C. Thereafter, the samples were centrifuged (12000 × *g*, 10 min, 4 °C) to collect the protein fraction (pellet; the supernatant was discarded), which was washed using two volumes of methanol, with centrifugation (12000 × *g*, 10 min, 4 °C) between each wash. Finally, an air flow in a fume hoof was used to dry the cleaned pellets for 1 h, which were the dissolved in 100 µL of shotgun buffer (8 M urea, 2 M thiourea, 0.15% AALS II in 100 mM tris-HCl, pH 7.5). A 2-D Quant Kit (GE Healthcare, San Francisco, CA, USA) was used to determine the protein contents [26]

Proteins extracted as described above (100 µg) were trypsinized according to the filter aided sample preparation (FASP) protocol. Reduction buffer (100 mM dithiothreitol (DTT), 8 M urea, 100 mM tetraethylammonium tetrahydroborate (TEAB), pH 8.0; 120 µL) was added to the sample, which was incubated for 1 h at 60 °C. Indole acetic acid (IAA; final concentration 50 m) was then added and the solution was incubated for 40 min in the dark at room temperature. Next, the proteins were digested and then subjected to centrifugation at 10,000 × g at 4 °C for 20 min; the flowthrough was discarded from the collection tube. Then, TEAB (100 mM, 100 µL), followed by sequencing-grade trypsin (2 µL: 1 µg), was added to each tube followed by incubation for 12 h at 37 °C. Finally, the digested peptides were subjected to centrifugation at 10,000 × *g* for 20 min. TEAB (100 mM, 50 µL) was added and the preparation was recentrifuged, lyophilized, and stored at −80 °C. For isobaric tags for relative and absolute quantitation (iTRAQ) labeling, 100 µL of iTRAQ reagent was added to each sample, and 40 µL of the resultant samples were used for labeling. Next, 100 µL iTRAQ reagent was added, vortexed, and incubated for 2 h at room temperature. Finally, the reaction was terminated by adding 200 µL of water, lyophilized, and stored at −80 °C [27].

2.5 LC-MS/MS and Bioinformatic Analyses

An Agilent 1100 HPLC System (Agilent Technologies Inc., Santa Clara, CA, USA) with an Agilent Zorbax Extend RP column (5 µm, 150 mm × 2.1 mm) as used for reversed-phase (RP) separation. RP separation was conducted using mobile phase A (2% acetonitrile in HPLC-grade water) and B (98% acetonitrile in HPLC-grade water) according to the following scheme: 98% A for 0 − 8 min; 98 − 95% A for 8.00 − 8.01 min; 95 − 75% A for 8.01 − 38 min; 75 − 60% A for 48 − 60 min; 60 − 10% A for 60 − 60.01 min; 10% A for 60.01 − 70 min; 10 − 98% A for 70 − 70.01 min; and 98% A for 70.01 − 75 min. A fluent flow rate of 300 $\mu L \cdot min^{-1}$ was used to separate the tryptic peptides, with monitoring at 210 and 280 nm. The eluate was collected each minute and numbered from 1 to 10 within the pipeline. For MS detection, the separated peptides were lyophilized.

According to the method of Cao et al., LC-MS/MS was carried out using Thermo Easy-nLC 1200 coupled Q Exactive mass spectrometry, with slight modifications [28]. An autosampler was used to load the samples onto a trap column (100 µm × 20 mm; PEP Map C18), which were then separated at a flow rate of at 300 $nL \cdot min^{-1}$ using an analysis column (75 µm × 150 mm; PEP Map C18).

Buffer A (0.1% formic acid in water) and buffer B (0.1% formic acid in acetonitrile) comprised the mobile phase. The linear washing gradient comprised: 4% buffer B for 0–7 min; 4–25% B for 8–51 min; 25–40% B for 52–60 min; 40–85% B for 61–70 min; and 85% B for 71–74 min. Full MS scans were gained over

the mass range of 375–1800 m/z with a maximum injection time of 50 ms, an automatic gain control (AGC) target value of 4×10^5, and a mass resolution of 120,000 (at m/z 200). Dynamic exclusion, run in positive mode, was set to 60.0 s. The 10 most intense MS peaks were subjected to fragmentation using higher-energy collisional dissociation at a collision energy of 30 eV. Using a maximum injection time of 50 ms, MS/MS spectra were obtained at 17,500 (at m/z 200) resolution. To search the raw fusion data against the sample protein database, we used Proteome Discoverer (v.2.2, Thermo Fisher Scientific, Waltham, MA, USA).

Hierarchical clustering analysis (HCA) and global heat maps were used to exhibit the differentially abundant proteins. The Omicsbean resourse should be references as [29].

2.6 Western blotting

Briefly, a 20-μg sample of ileum protein was electrophoresed through precast polyacrylamide gels (Bio-Rad, Hercules, CA, USA). The separated proteins were then transferred onto polyvinylidene fluoride membranes at 4 °C overnight. Thereafter, either 5% (w/v) BSA in Tris-buffered saline with 0.1% (v/v) Tween 80 (TBS-T) or 5% (w/v) skim milk in TBS-T were used to block the membranes. The membranes were then incubated with primary antibodies recognizing FgA, FgG, FgB, and C3, followed by incubation with the appropriate horseradish peroxidase-labeled secondary antibodies (Cell Signaling Technology, Danvers, MA, USA). Enhanced chemiluminescence detection reagents (Thermo Fisher Scientific) were used to visualize the immunoreactive protein bands. GeneTools 4.3.8 (Syngene, Cambridge, UK) was used for densitometry analysis. To correct for variations in protein loading and transfer efficiency, amido black total protein staining was performed.

2.7 Statistical considerations

GraphPad Prism software version 8 for Windows (GraphPad Software, La Jolla, CA, USA). IBM SPSS Statistics 26 (IBM Corp., Armonk, NY, USA) was used to calculate and analyze the data. A p value less than 0.05 was considered to indicate statistical significance.

3. Results

3.1 GRg1's antidiarrheal effect on ETEC-infected mice

As shown in Table 2, compared with the Normal group, the diarrhea index of the Model group increased significantly ($P < 0.05$). The diarrhea index of the Model group showed a significant difference with that of the three GRg1 groups ($P < 0.05$); however, there was no significant difference among the three GRg1 dose groups ($P > 0.05$), indicating that GRg1 has a therapeutic effect on ETEC-induced diarrhea, but without significant dosedependence.

3.2 Effects of GRg1 on plasma inflammatory mediators and markers in mice with ETEC diarrhea

Figure 1 shows that the plasma levels of TNFα, IL1β, and IL6 in the Model group were significantly higher compared with those of the Normal group, which indicated a strong inflammatory reaction after ETEC

infection. However, the levels of these inflammatory mediators and markers decreased significantly under all three doses of GRg1, with no significant dose-dependent effect.

Table 2
Treatment method and diarrhea index of the mice in each group.

Group	GRg1(mg/kg)	ETEC	Diarrhea index
Normal	-	-	1.28 ± 0.22^{a}
Model	-	+	2.16 ± 0.39^{b}
LD	50	+	1.49 ± 0.34^{a}
MD	100	+	1.37 ± 0.30^{a}
HD	150	+	1.33 ± 0.35^{a}
Note: Values are represented as the mean ± standard deviation, n = 12, and values with no letter or the same letter superscripts mean no significant difference ($P > 0.05$), while those with different letter superscripts indicate a significant difference ($P < 0.05$).			

3.3 GRg1's effects on the intestinal morphology of mice with ETEC diarrhea

In the Normal group, the ileum structure was intact, and almost no inflammatory cells were seen; in the Model group, obvious inflammatory cell infiltration (red arrow) was found in the ileum, and the villi structure was seriously damaged (blue arrow). This indicated that ETEC infection caused severe inflammation in the ileum of the mice, and damaged the villi, which would affect the physiological function of the ileum. However, histological observation of the ileum of mice treated with GRg1 at different doses showed that significantly less villi damage and fewer inflammatory cells than in the Model group, indicating that GRg1 could alleviate the inflammation caused by ETEC infection and maintain the ileal structure under attack by ETEC (Fig. 2).

The results of HE staining are shown in Fig. 3. In the Model group, the villus height and crypt depth were significantly lower compared with those in the Normal group ($P < 0.05$). In the three GRg1 treatment groups, the villus height and crypt depth were significantly higher compared with those in the Model group ($P < 0.05$). However, among the three doses of GRg1, there was no significant difference in the villus height and crypt depth, indicating that GRg1 can maintain the morphology and structure of duodenum in ETEC infection, without obvious dose-dependency.

3.4 Differentially abundant proteins detected using proteomics

The criteria of fold change ≥ 1.3 or fold change ≤ 0.77, and $p < 0.05$ were used to identify significant differentially abundant proteins in each treatment group compared with the Model group, respectively. According to previous results, we judged that the effect of GRg1 on ETEC diarrhea was not dose-dependent within the range tested, so we selected the common differentially abundant proteins between

the three GRg1 treatment groups and Model group for analysis. This analysis showed that the levels of 55 proteins changed significantly in all three GRg1 treatment groups. Seven proteins were significantly upregulated and 48 proteins were significantly downregulated (Supplementary Table). Hierarchical cluster analysis (HCA) was used to cluster the samples (Fig. 4).

3.5 Common pathway analysis

In KEGG pathways enrichment analysis, the 55 differentially abundant common proteins were identified as being associated with 15 enriched pathways. The differentially abundant proteins were mainly associated with complement and coagulation cascades (five proteins), platelet activation (three proteins), fat digestion and absorption (three proteins), pancreatic secretion (three proteins), *Staphylococcus aureus* infection (three proteins) (Fig. 5).

3.6 Western Blotting

Western blotting was performed to validate the proteomic results on the same experimental low-dose samples for a subset of proteins. Complement and coagulation cascades pathway and the platelet activation pathway were identified as two key signaling pathways in the KEGG pathways enrichment analysis, and have important functions during the middle stage of the inflammatory response. Four differentially abundant proteins from these two signaling pathways were selected for western blotting verification: C3, FgA, FgB, and FgG. These four proteins are involved in the complement and coaggregation cascades pathway, and FgA, FgB and FgG are also key proteins in the platelet activation pathway.

According to Fig. 6, compared with that in the Model group, the level of C3 in ileum of mice treated with GRg1 at the three doses decreased by 27.37, 33.42, and 44.61%; FgA decreased by 27.42, 25.45, and 37.06%; FgB decreased by 35.75, 33.15, and 52.07%; and FgG decreased by 65.15, 60.15, and 60.70%, respectively ($P < 0.05$). In addition, for the levels of these proteins, there was no significant difference between the different doses of GRg1 treatment ($P > 0.05$). These results indicated that GRg1 significantly inhibited the expression of the above four proteins in the ileum of ETEC diarrhea mice in a doseindependent manner, which was consistent with proteomic results.

4. Discussion

In recent years, GRg1, as a substitute for traditional antibiotics or as an anti-inflammatory drug, has attracted extensive research interest. The tetracyclic triterpenoid derivative GRg1 is derived from a dammarane hydride. GRg1 affects the immune, blood, cardiovascular, and nervous, systems, demonstrating a variety of pharmacological effects [30, 31]. *Escherichia coli* diarrhea in farm animals is commonly caused by ETEC [32]. Characteristically, ETEC produce two kinds of virulence factors: enterotoxins that induce fluid secretion and adhesins that encourage the binding and colonization of the intestinal epithelium [33]. Enterotoxins cause apoptosis of endothelial cells, destroy tight junctions, and induce inflammation of the intestinal mucosa [3, 34]. The present study determined the effect of different GRg1 doses on ETEC diarrhea. The results showed that the three doses of GRg1 could significantly

reduce the diarrhea index (used as the evaluation standard of the degree of diarrhea) of ETEC diarrhea mice, which indicated that GRg1 had a marked anti-ETEC diarrhea effect, and there was no dose dependence in the range of 50–150 mg / kg.

To study the mechanism of prevention of ETEC diarrhea by GRg1, we first compared the intestinal morphology of mice with ETEC diarrhea and the infected mice treated with GRg1. In the intestinal tract, villi are vital components, whose structure can be used to indicate the small intestines' absorptive capacity [35]. To assess intestinal morphology, crypt depth and villus height are commonly used as metrics [35]. Gut health is reflected by intestinal morphology to some extent. Deeper crypts and shorter villi might indicate that the intestinal tract has a decreased surface area for nutrient uptake. Our results showed that the ileal villus height and crypt depth were significantly decreased in ETEC-infected mice, accompanied by ocular cell infiltration, indicating that ETEC severely impaired the integrity of the ileal structure, which supported the conclusions of previous studies, who reported that ETEC-secreted toxins were closely associated with small intestine morphological alterations [37, 38] However, the ileal villus height and crypt depth of GRg1-treated mice were significantly higher than those of the Model group, and the number inflammatory cells decreased significantly, indicating that GRg1 could maintain ileal morphology, had an anti-inflammatory effect, and showed no dose dependence in the range of 50–150 mg/kg.

In the body's cellular immunity, cytokines are important, playing vital roles in lymphocyte development and the subsequent function of the peripheral immune compartment [39]. The strong pro-inflammatory cytokine, TNFα (also known as cachectin), has an important immune system function during apoptosis, cell differentiation, cell proliferation, and inflammation [39]. In 1975, Carwell et al. first described TNFα as a cytokine with significant cytotoxic activity in a stimulated immune system, thus causing tumor necrosis. In 1984, the gene encoding TNFα was cloned, which revealed structural homology with lymphotoxin (LT)-a; therefore, TNFα was added to the cytokines in the TNF ligand superfamily [41]. The soluble protein IL6 has a pleiotropic effect on hematopoiesis, the immune response, and inflammation, and is produced promptly and transiently in response to tissue injury and infection. IL6 stimulates immune reactions, hematopoiesis, and acute phase responses, thereby contributing to host defense. Transcriptional and posttranscriptional mechanisms control IL6 expression strictly; however, constitutive expression of IL-6 has a pathological effect on autoimmunity and chronic inflammation [42, 43]. The potent proinflammatory cytokine IL1β is vital for host-defense responses to injury and infection [44]. Among the 11 IL1 family members, IL1β is the best studied and characterized. Although various cell types produce and secrete IL1β, the overwhelming majority of studies have dealt with its production from innate immune system cells, especially macrophages and monocytes [45]. Therefore, the important proinflammatory cytokines TNFα, IL6, and IL1β regulate the immunity of the host to various pathogens via immune cell differentiation, proliferation, and apoptosis [46]. However, the body can be damaged by excessive pro-inflammatory cytokine production [47].

After ETEC challenge, the mouse plasma concentrations of TNFα, IL6, and IL1β were elevated, which suggested the presence of an acute inflammatory response, and was consistent with a previous reports

[47]. These results verified that the model was constructed successfully. Interestingly, serum IL6 and TNFα levels decreased significantly in ETEC stimulated mice treated with GRg1, which suggested that GRg1 might prevent ETEC diarrhea by negatively regulating the inflammatory response.

Under threat from damaging external stimuli, such as chemical toxins and microbial infections, the body mounts a complex inflammatory response [47]. Characteristically, the inflammatory response comprises a number of steps, such as coordinated signaling pathways activation; proinflammatory cytokines, chemokines, and adhesion molecules expression in resident tissue cells, and leukocyte (mainly macrophages, neutrophils and dendritic cells) and inflammatory mediator infiltration from the vascular system, inducing the removal of the harmful stimuli and the initiation of healing. However, excessive inflammation can cause diseases in animals [50, 51]. To gain insights into the mechanisms by which GRg1 regulates the inflammatory response, we used proteomics to explore the differentially abundant proteins in the ileum of ETEC-infected mice treated with and without GRg1. Our preliminary results showed that in the dose range of 50–150 mg/kg, GRg1 could prevent ETEC diarrhea in a dose-independent manner; therefore, we selected the common differential proteins in the three treatment groups for analysis. As a result, compared with the Model group, we identified 55 differentially abundant proteins (seven upregulated and 48 downregulated). In KEGG pathways enrichment analysis, the differentially abundant proteins were enriched in 15 pathways. Among them, we were most interested in the signaling pathways, namely “complement and coagulation cascades” and “platelet activation”, which are closely related to the inflammatory response. We verified the key differential proteins in these two signaling pathway: C3, FgA, FgB, and FgG, using western blotting. These four proteins are important proteins in the completion and coagulation cascade signaling pathways, and FgA, FgB, and FgG also regulate the platelet activation pathway. The results showed that these four proteins were significantly downregulated after GRg1 treatment, which was consistent with the results of proteomics. C3 regulates both the alternative and classical complement pathways [52], and complement system activation aids the adaptive immunity system to eliminate foreign pathogens more effectively. C3 also has strong chemoattractant properties, allowing it to guide certain immune cells to the complement activation sites. Inflammatory and coagulatant responses, and the promotion of tissue damage, are further amplified via complement system activation [53]. Consequently, host organ and tissue damage can occur in response to excessive activation of the coagulation, complement, and inflammatory systems, even resulting in multiple organ failure and death [54]. FgA, FgB, and FgG are fibrinogens, which also participate in platelet activation as regulatory proteins. Inflammation and coagulation are interconnected and recent studies have demonstrated a direct role of platelets in a variety of inflammatory processes [55–57], which is not the traditional view of platelets. However, not only were platelets shown to have are direct inflammatory role, but also were demonstrated as coagulation cascade members that interact with inflammatory mediators in a complex, yet important, manner. The activation and localization of the complement cascade is just one of the functions exerted by platelets during inflammation. In the present study, under infection of ETEC, C3, FgA, FgB, and FgG levels in the ileum of mice were downregulated by varying degrees after GRg1 treatment. This suggested that GRg1 can inhibit the complement and coagulation cascade pathway to some extent by downregulating the abundance of these key proteins, thus reducing

the inflammatory reaction. In addition, downregulation of FgA, FgB, and FgG levels also inhibited the platelet activation pathway and further reduced the inflammatory response. In other words, GRg1 prevents ETEC diarrhea by inhibiting inflammation-related signaling pathways in the mouse ileum.

5. Conclusion

GRg1 treatment for 14 days could maintain the integrity of the ileum mucosa and downregulate the inflammatory factors in serum during ETEC infection. It inhibit inflammation-related pathways by downregulating the levels of C3, FgA, FgB, and FgG in the ileum, thus preventing ETEC induced diarrhea in mice. In addition, there was no dose dependence in the range of 50–150 mg/kg.

List Of Abbreviations

Abbreviation	Full name
ETEC	Enterotoxigenic *Escherichia coli*
GRg1	Ginsenoside Rg1
IL1β	Interleukin 1β
IL6	Interleukin
TNFα	Necrosis factor alpha
ADRs	Adverse drug reactions
HPLC	High performance liquid chromatography
CICC	China Center of Industrial Culture Collection
FgA	Fibrinogen alpha chain
FgB	Fibrinogen beta chain
FgG	Fibrinogen gamma chain
C3	Complement 3
NIH	National Institutes of Health
H & E staining	Hematoxylin and eosin staining
PMSF	Phenylmethylsulfonyl fluoride
FASP	Filter aided sample preparation
IAA	Indole acetic acid
DTT	Dithiothreitol
iTRAQ	Isobaric tags for relative and absolute quantitation
RP	Reversed-phase
AGC	Automatic gain control
HCA	Hierarchical clustering analysis

Declarations

Ethics approval and consent to participate

This research has been granted by the Animal Protection and Use Committee of South China Agricultural University and complied with Ethical Standards

Consent for publication

This research including all the paper detail, data, tables and images was consented by all the authors and respondents in this paper for publication. And they will be freely available on the internet.

Availability of data and materials

Data supporting the results can be found in this paper. The datasets generated during and analyzed during the current study are available from the corresponding author on reasonable request.

Authors' contributions

Jian Kang: protocol designing, data collecting and analyzing, paper writing.Qin Ai: data collecting.Yan-Hong Zhou: data collecting. Chun-Yang Zhu: data collecting. Bing-Hu Fang: protocol designing, data collecting and analyzing, paper writing. All authors read and approved the final manuscript.

Competing Interests

The authors declare that they have no competing interests.

Funding

This work is supported by the 13th five-year plan for national key research (grant number: 2016yfd0501308). The funding body had no role in the design of the study, in the collection, analysis, and interpretation of data, and in writing the manuscript.

Acknowledgements

We would like to thank the native English speaking scientists of Elixigen Company (Huntington Beach, California) for editing our manuscript

References

[1]. Béla N Péter Zs. Fekete. Enterotoxigenic Escherichia coli in veterinary medicine. J Med Microbiol. 2005; 295(6-7): 443-54.

[2]. Sack RB. Human Diarrheal Disease Caused by Enterotoxigenic Escherichia Coli. Annu Rev Microbiol. 1975; 29: 333-53.

[3]. Heinfried S, Andreas S, Ruth W, Alfons B, Hubert B, Martha MG, et al. Effect of Endotoxemia on Intestinal Villus Microcirculation in Rats. J Surg Res, 1996; 61(2): 521-6.

[4]. Gupta M Kumar A. Comparison of Minimum Inhibitory Concentration (MIC) value of statin drugs: A Systematic Review. Anti-Infective Agents. 2019; 17: 4-19.

[5]. Benhamou RI, Shaul P, Herzog Ido M., Fridman M. Di-N-Methylation of Anti-Gram-Positive Aminoglycoside-Derived Membrane Disruptors Improves Antimicrobial Potency and Broadens Spectrum

to Gram-Negative Bacteria. Angew Chem Int Edit. 2015; 54(46): 13617-21.

[6]. Govindappa PK, Gautam V, Tripathi SM, Sahni YP, Raghavendra HLS. Effect of Withania somnifera on gentamicin induced renal lesions in rats. Rev Bras Farmacogn, 2019. doi: 10.1016/j.bjp.2018.12.005.

[7]. Gupta M, Sharma R, Kumar A. Comparative potential of Simvastatin, Rosuvastatin and Fluvastatin against bacterial infection: an in silico and in vitro study. Orient Pharm Exp Med. 2019. doi: 10.1007/s13596-019-00359-z.

[8]. Ritika R, Ruchika S, Anoop K. Repurposing of Existing Statin drugs for treatment of Microbial Infections: How much Promising? Infect Disord Drug Targets. 2019; 19(3): 224-237.

[9]. Yachika K, Ruchika S, Anoop K. Repurposing of existing drugs for the bacterial infections: An In silico and In vitro study. Infect Disord Drug Targets. 2020; 20(2):182-197.

[10]. Li J, Liu D, Wu JF, Zhang D, Cheng BB, Zhang, YN, et al. Ginsenoside Rg1 attenuates ultraviolet B-induced glucocortisides resistance in keratinocytes via Nrf2/HDAC2 signalling. Sci Rep. 2016. doi: 10.1038/srep39336.

[11]. Yao X, Jiang W, Ma CH, Yu DH, Zhu JG, Cheng ZQ, Bao JA. Protective effects of Ginsenoside Rg1 against carbon tetrachloride-induced liver injury in mice through suppression of inflammation. Phytomedicine. 2016; 23(6): 583-8.

[12]. Ma SW, Benzie IFF, Chu TTW, Fok BSP, Tomlinson B, Critchley LAH. Effect of Panax ginseng supplementation on biomarkers of glucose tolerance, antioxidant status and oxidative stress in type 2 diabetic subjects: results of a placebo-controlled human intervention trial. Diabetes Obes Metab. 2008; 10(11): 1125-7.

[13]. Yang X, Wu, XZ. Main Anti-tumor Angiogenesis Agents Isolated From Chinese Herbal Medicines. Mini Rev Med Chem. 2015;15(12): 1011-23.

[14]. Liu CX, Xiao PG. Recent advances on ginseng research in China. J Ethnopharmacol. 1992; 36(1): 27-38.

[15]. Kim JH, Yi YS, Kim MY, Cho JY. Role of ginsenosides, the main active components of Panax ginseng, in inflammatory responses and diseases. J Ginseng Res. 2017; 41(4): 435-443.

[16]. Jin C, Wang ZZ, Zhou H, Lou YX, Zhang DS. Ginsenoside Rg1-induced antidepressant effects involve the protection of astrocyte gap junctions within the prefrontal cortex. Prog Neuropsychopharmacol Biol Psychiatry. 2017; 75: 183-191.

[17]. Gao Y, Chu SF, Zhang Z, Chen NH. Hepataprotective effects of ginsenoside Rg1-A review. J Ethnopharmacol. 2017; 206: 178-183.

[18]. Tian W, Chen L, Zhang L, Wang B, Li XB, Fan KR, et al. Effects of ginsenoside Rg1 on glucose metabolism and liver injury in streptozotocin-induced type 2 diabetic rats. Genet Mol Res. 2017; 16(1). doi: 10.4238/gmr16019463.

[19]. Gao Y, Chu SF, Shao QH, Zhang MJ, Xia CY, Wang YY, et al. Antioxidant activities of ginsenoside Rg1 against cisplatin-induced hepatic injury through Nrf2 signaling pathway in mice. Free Radic Res. 2017; 51(1): 1-13.

[20]. Gao Y, Chu SF, Zhang Z□Zuo W, Xia CY, Ai QD, et al. Early Stage Functions of Mitochondrial Autophagy and Oxidative Stress in Acetaminophen-Induced Liver Injury. J Cell Biochem. 2017; 118(10): 3130-3141.

[21]. Gao Y, Chu SF, Xia CY, Zhang Z, Zhang S, Chen NH. Rg1 Attenuates alcoholic hepatic damage through regulating AMP-activated protein kinase and nuclear factor erythroid 2-related factor 2 signal pathways. J Asian Nat Prod Res. 2016;18(8): 765-78.

[22]. Gao Y, Chu SF, Li JW, Li JP, Zhang Z, Xia CY, et al. Anti-inflammatory function of ginsenoside Rg1 on alcoholic hepatitis through glucocorticoid receptor related nuclear factor-kappa B pathway. J Ethnopharmacol. 2015; 173: 231-40.

[23]. Sun XC, Ren XF, Chen L, Gao XQ, Xie JX, Chen WF. Glucocorticoid receptor is involved in the neuroprotective effect of ginsenoside Rg1 against inflammation-induced dopaminergic neuronal degeneration in substantia nigra. J Steroid Biochem Mol Biol. 2016; 155(Pt A): 94-103.

[24]. Zhang LM, Zhu MJ, Li MM, Du Y, Fu FH. Ginsenoside Rg1 attenuates adjuvant-induced arthritis in rats via modulation of PPAR-γ/NF-κB signal pathway. Oncotarget. 2017; 8(33): 55384-55393.

[25]. Li YJ, Zhang GY, Chen ML, Tong M, Zhao M, Tang F, et al. Rutaecarpine inhibited imiquimod-induced psoriasis-like dermatitis via inhibiting the NF-κB and TLR7 pathways in mice. Biomed Pharmacother. 2019; 109: 1876-1883.

[26]. Wong SY, Hashim OH, Hayashi N. Development of high-performance two-dimensional gel electrophoresis for human hair shaft proteome. PLoS ONE. 2019; 14(3): e0213947.

[27]. Liu CW, Zhang QB. Isobaric Labeling-Based LC-MS/MS Strategy for Comprehensive Profiling of Human Pancreatic Tissue Proteome. Methods Mol Biol. 2018; 1788: 215-224.

[28]. Cao JY, Xu YP,Cai XZ. TMT-based quantitative proteomics analyses reveal novel defense mechanisms of Brassica napus against the devastating necrotrophic pathogen Sclerotinia sclerotiorum. J Proteomics. 2016; 143:265-277.

[29]. Omicsbean online bioinformatics resource. http://www.omicsbean.cn/. Accessed 12 June 2019.

[30]. Lee YJ, Chung E, Lee KY, Lee YH, Lee SK. Ginsenoside-Rg1, one of the major active molecules from Panax ginseng, is a functional ligand of glucocorticoid receptor. Mol Cell Endocrinol. 1997; 133(2): 135-140.

[31]. Fang HE, Yu LM. Effects of ginsenoside Rg1 on characteristics and functions of adult stem cells. Chinese Pharmacological Bulletin. 2016; 32(03): 319-322.

[32]. Béla N, Péter Zs. Fekete. Enterotoxigenic Escherichia coli in veterinary medicine. Int J Med Microbiol. 2005; 295(6-7): 443-54.

[33]. Kopic S, Geibel JP. Toxin mediated diarrhea in the 21 century: the pathophysiology of intestinal ion transport in the course of ETEC, V. cholerae and rotavirus infection. Toxins (Basel). 2010; 2(8): 2132-57.

[34]. Dubreuil JD. The whole Shebang: the gastrointestinal tract, Escherichia coli enterotoxins and secretion. Curr Issues Mol Biol. 2012; 14(2): 71-82.

[35]. Caspary WF. Physiology and pathophysiology of intestinal absorption. Am J Clin Nutr. 1992; 55(1 Suppl): 299S-309S.

[36]. Liu Y, Chen F, Odle J, Lin X, Jacobi SK, Zhu H, et al. Fish oil enhances intestinal integrity and inhibits TLR4 and NOD2 signaling pathways in weaned pigs after LPS challenge. J Nutr. 2012; 142(11): 2017-24.

[37]. Gíslason J，Suhasini Iyer ，Hutchens TW，LONNERDAL B. Lactoferrin receptors in piglet small intestine: Lactoferrin binding properties, ontogeny, and regional distribution in the gastrointestinal tract. J Nutr Biochem. 1993; 4(9): 528-533.

[38]. Trier, Jerry S. Mucosal flora in inflammatory bowel disease: Intraepithelial bacteria or endocrine epithelial cell secretory granules? Gastroenterology. 2002; 123(3): 956.

[39]. He YW, Malek TR. The structure and function of gamma c-dependent cytokines and receptors: regulation of T lymphocyte development and homeostasis. Crit Rev Immunol. 1998; 18(6): 503-24.

[40]. Baud V, Karin M. Signal transduction by tumor necrosis factor and its relatives. Trends Cell Biol. 2001; 11(9): 372-377.

[41]. Wajant H, Pfizenmaier K, Scheurich P. Tumor necrosis factor signaling. Cell Death Differ. 2003; 10(1): 45-65.

[42]. Tanaka T, Narazaki M, Kishimoto T. IL-6 in Inflammation, Immunity, and Disease. Cold Spring Harb Perspect Biol. 2014; 6(10): a016295.

[43]. Kishimoto T. Factors Affecting B-Cell Growth and Differentiation. Annu Rev Immunol. 1985; 3: 133-57.

[44] Dinarello CA. Biologic basis for interleukin-1 in disease. Blood. 1996; 87(6): 2095-147.

[45]. Gloria LC, David B. Understanding the mechanism of IL-1β secretion. Cytokine Growth Factor Rev. 2011; 22(4): 189-195.

[46]. Lee, SH, Lillehoj HS, Jang SI, Lillehoj EP, Min W, Bravo DM. Dietary supplementation of young broiler chickens with Capsicum and turmeric oleoresins increases resistance to necrotic enteritis. Br J Nutr. 2013; 110(5): 840-847.

[47]. McKay DM Baird AW. Cytokine regulation of epithelial permeability and ion transport. Gut. 1999; 44(2): 283-9.

[48]. Xiao Q, Zhang SJ, Yang C, Du RY, Huang WX. Ginsenoside Rg1 Ameliorates Palmitic Acid-Induced Hepatic Steatosis and Inflammation in HepG2 Cells via the AMPK/NF- κ B Pathway. Int J Endocrinol. 2019; 2019. doi: 10.1155/2019/7514802.

[49]. Gao Y, Li JT, Wang J, Li X, Zhang L. Ginsenoside Rg1 prevent and treat inflammatory diseases: A review. Int Immunopharmacol. 2020; 87: 106805.

[50]. Peter H, Jenny F, Tetsuhiko N, Rosalba S, Carolyn AC, Nancy HR. Lymphoid Tissue Homing Chemokines Are Expressed in Chronic Inflammation. Am J Pathol. 2000; 156(4): 1133-8.

[51]. Dinarello CA. Anti-inflammatory Agents: Present and Future. Cell. 2010; 140(6): 935-50.

[52]. Sacks SH., Zhou WD. The role of complement in the early immune response to transplantation. Nat Rev Immunol. 2012; 12(6): 431-42.

[53]. Robert SM, Zhu H, Narcis IP, Glenn P, Florea L. Complement inhibition decreases the procoagulant response and confers organ protection in a baboon model of Escherichia coli sepsis. Blood. 2010; 116(6): 1002-10.

[54]. Hotchkiss RS, Karl IE. The Pathophysiology and Treatment of Sepsis. N Engl J Med. 2003; 348(2): 138-50.

[55]. Wu Y. Contact pathway of coagulation and inflammation. Thromb J. 2015; 13: 17.

[56]. Shanmugavelayudam SK, Rubenstein, DA, Wei Y. Effects of physiologically relevant dynamic shear stress on platelet complement activation. Platelets. 2011; 22(8): 602-610.

[57]. Sarah H, Li C, Tony W, Berhane G, Wei Y, David AR. Platelet activation, adhesion, inflammation, and aggregation potential are altered in the presence of electronic cigarette extracts of variable nicotine concentrations. Platelets. 2016; 27(7): 694-702.

Figures

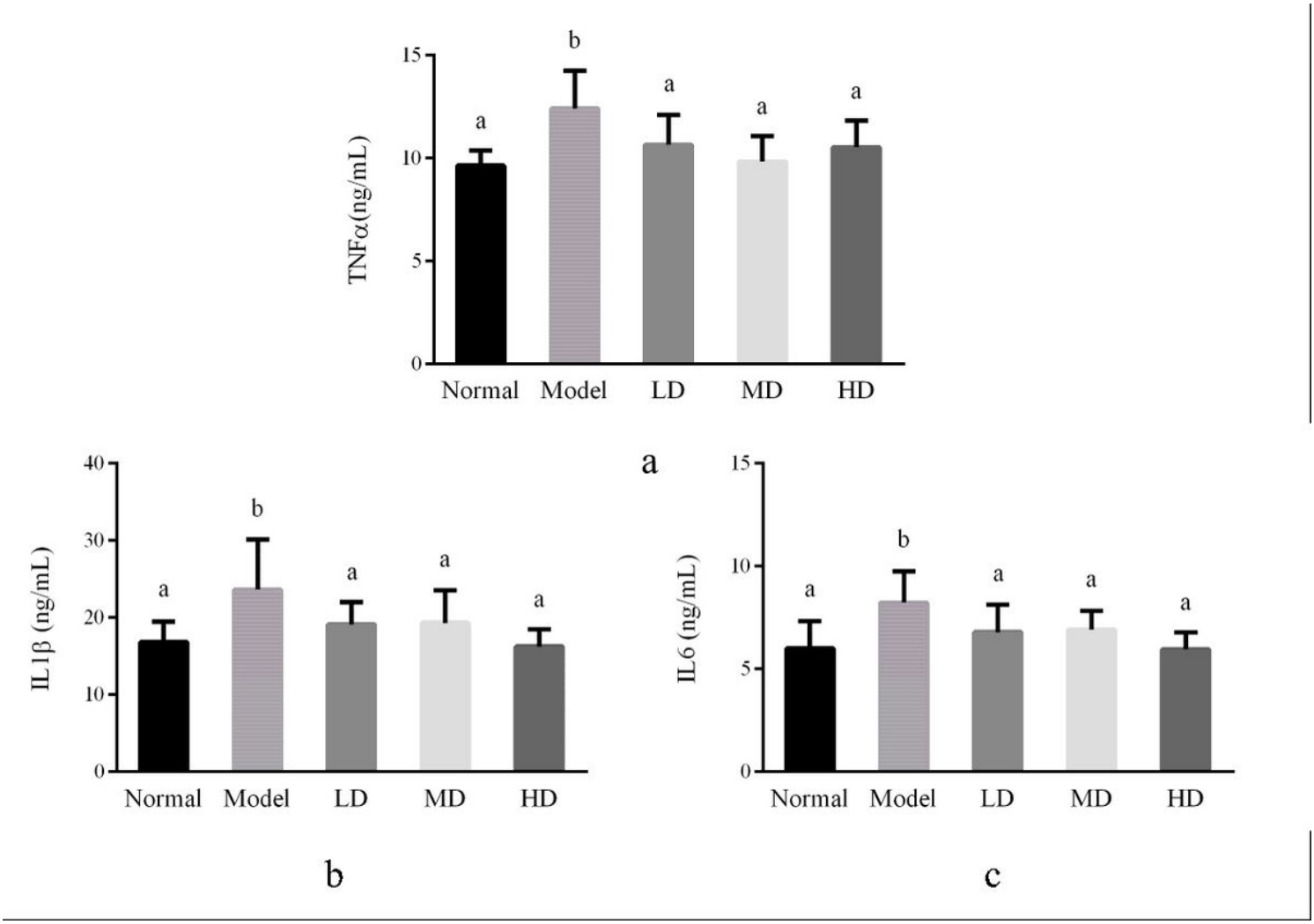

Figure 1

Effect of GRg1 on inflammatory mediators and markers in plasma: (a) TNFα levels in plasma. (b) IL1β levels in plasma. (c) IL6 levels in plasma. Values are represented as the mean ± standard deviation, n = 12. Values without a superscript letter or with the same superscript letter indicate no significant difference ($P > 0.05$); values with different superscript letters indicate significant differences ($P < 0.05$).

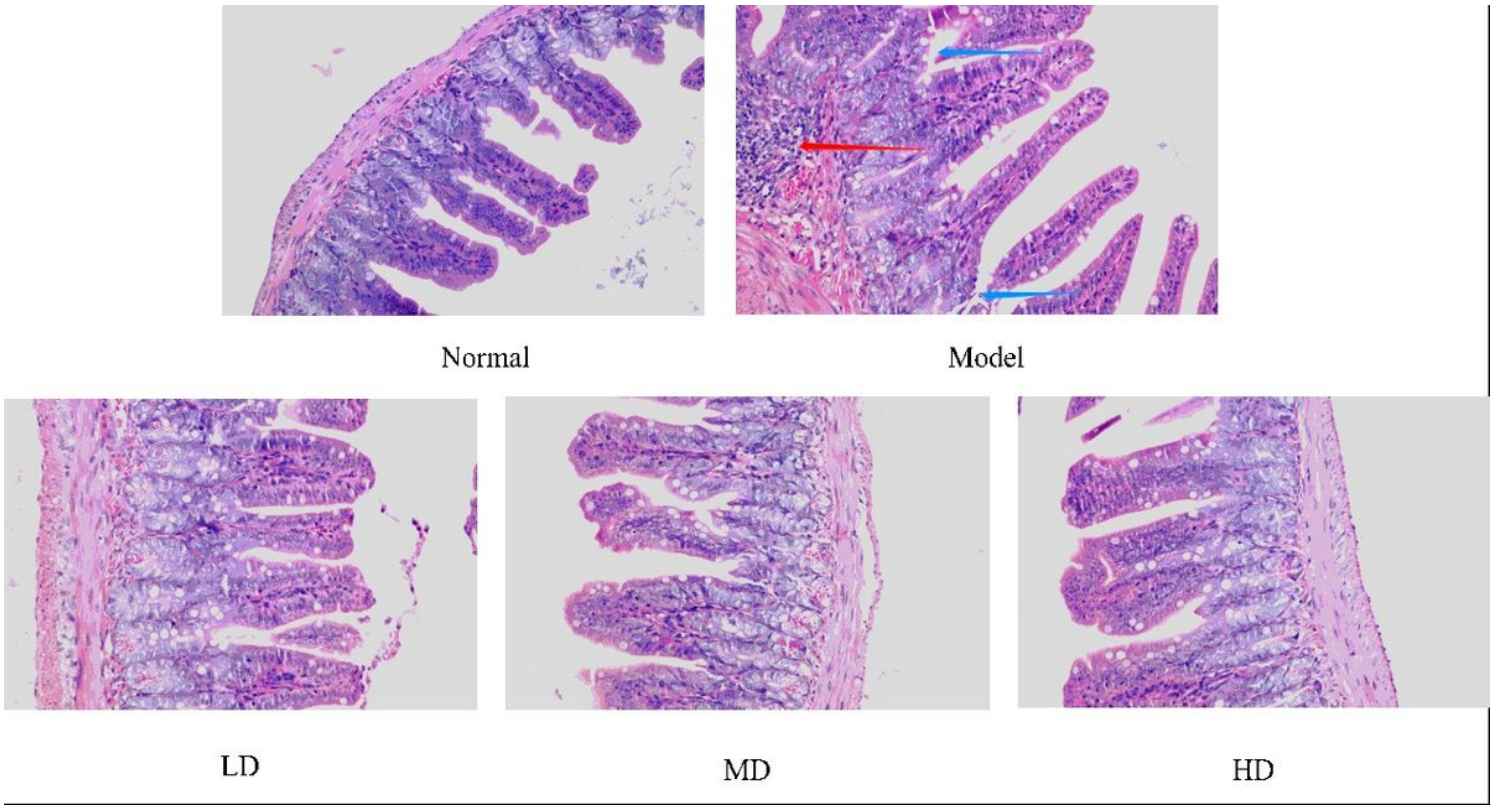

Figure 2

Images showing mouse ileums stained with hematoxylin and eosin to show any histopathological changes (200×). In the Normal group, the ileum structure was intact, and almost no inflammatory cells were seen; in the Model group, obvious inflammatory cell infiltration (red arrow) was found in the ileum, and the villi structure was seriously damaged (blue arrow). However, histological observation of the ileum in GRg1-treated mice at different doses showed significantly less villi damage and fewer inflammatory cells compared with those in the Model group.

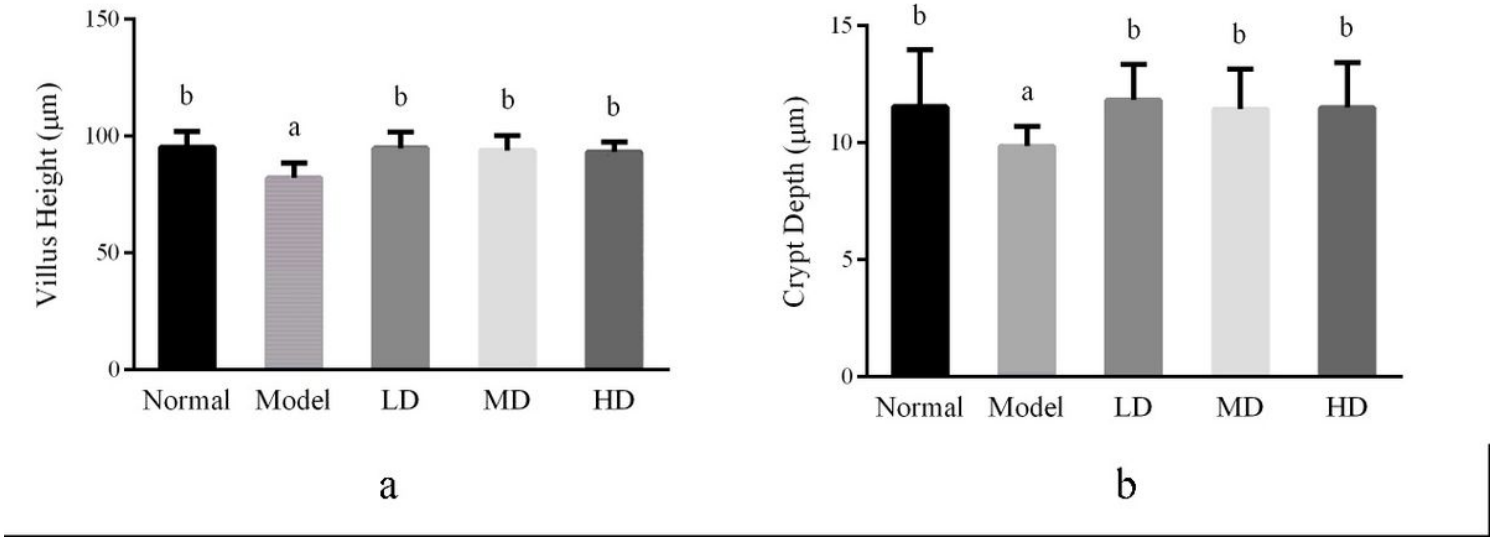

Figure 3

GRg1's effect on ileum morphology-related indexes: (a) Villi height. (b) Depth of crypt. Values are represented as the mean± standard deviation, n = 12. Values without a superscript letter or with the same superscript letter indicate no significant difference (P > 0.05); values with different superscript letters indicate significant differences (P < 0.05).

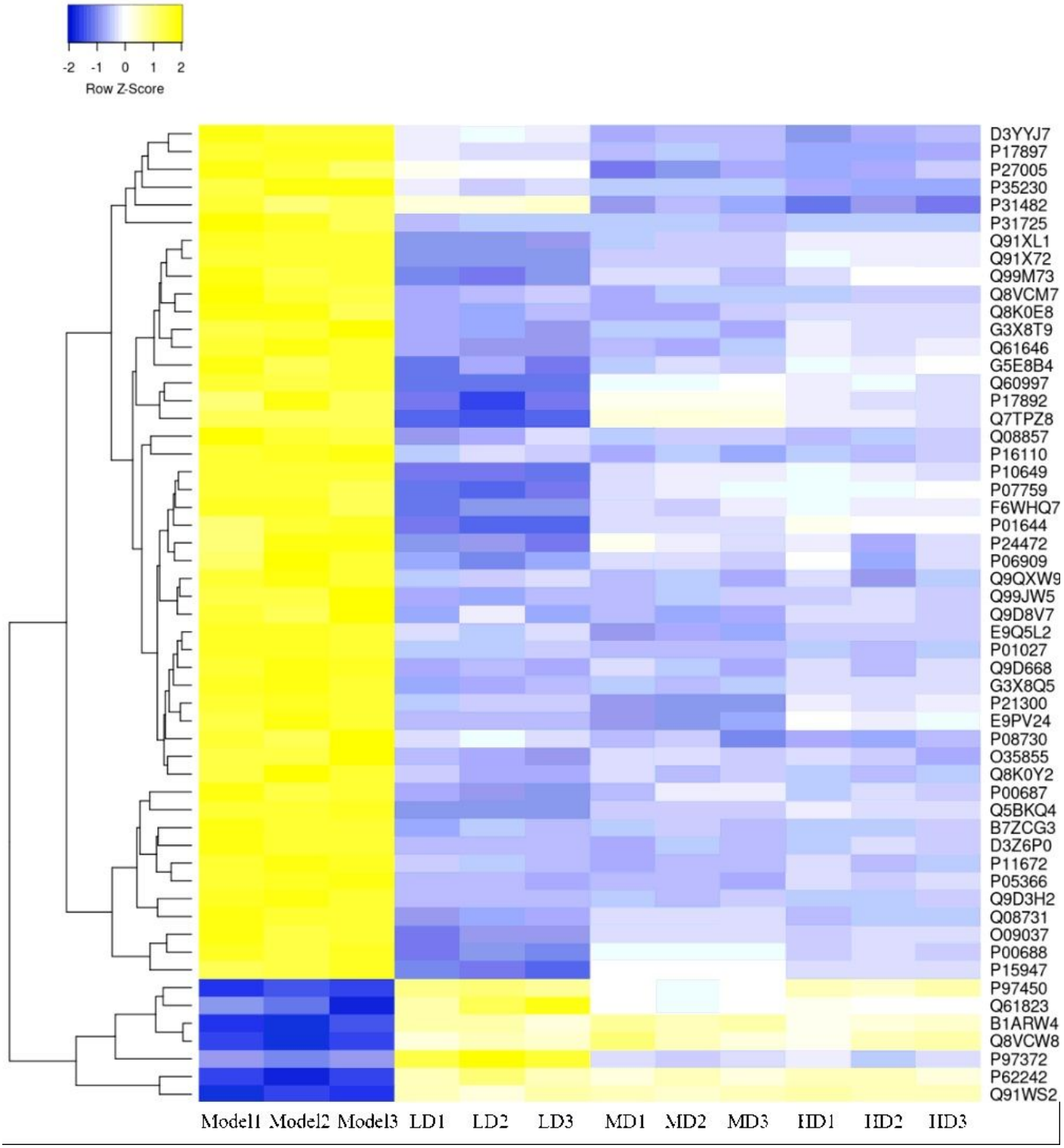

Figure 4

HCA analysis of differentially abundant proteins in LD, MD and HD groups compared with those in the Model group. Yellow indicates high abundance, whereas shades of blue represent lower abundance.

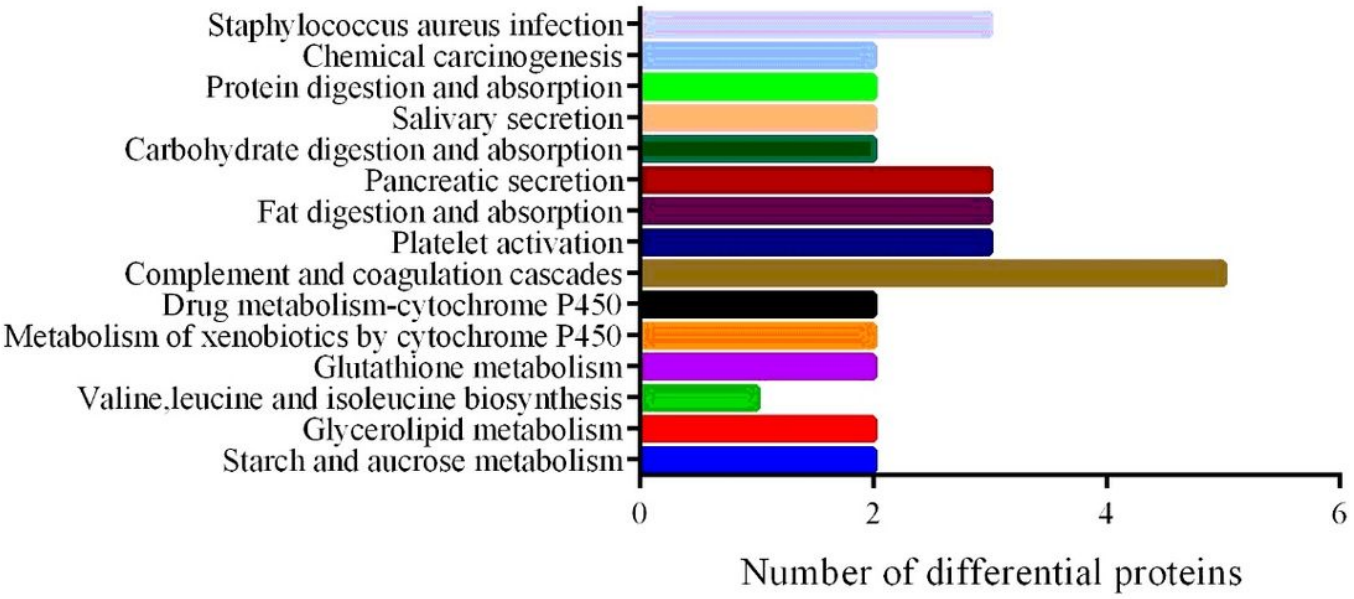

Figure 5

KEGG pathways enrichment of the 55 significantly differentially abundant proteins that were common among the three GRg1 groups

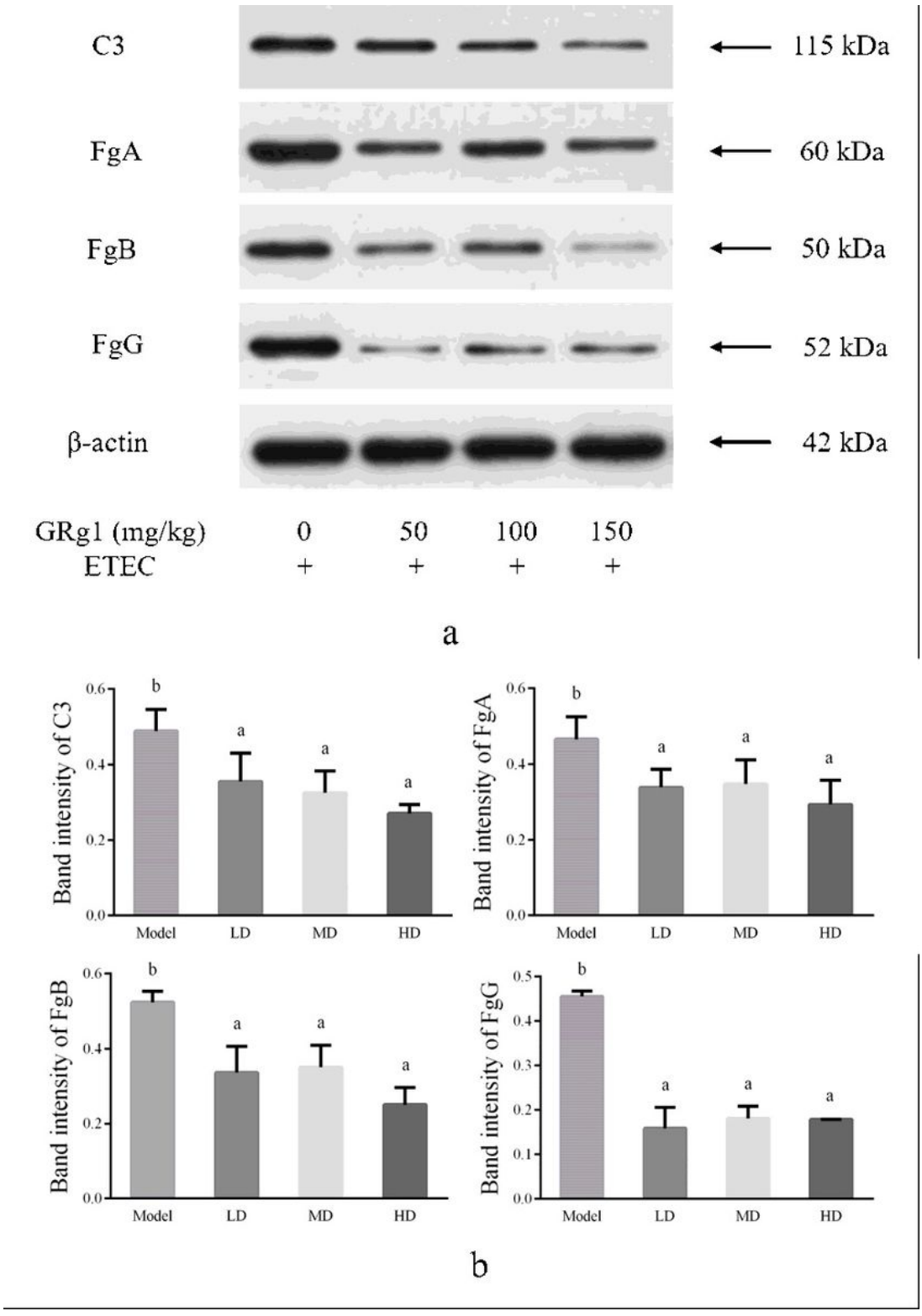

Figure 6

Effects of different doses of GRg1 on the C3, FgA, FgB, and FgG levels in mouse ileum. (a) Levels of C3, FgA, FgB, and FgG in ileum of the Model group and GRg1 treatment groups. (b) Quantified by means of the intensities of their bands. Values are represented as mean ± standard deviation, n=3. Values without a superscript letter or with the same superscript letter indicate no significant difference ($P > 0.05$); values with different superscript letters indicate significant differences ($P < 0.05$).

Supplementary Files

This is a list of supplementary files associated with this preprint. Click to download.

- SupplementaryTable.pdf